PLISKA
STUDIA MATHEMATICA
BULGARICA

ПЛИСКА
БЪЛГАРСКИ
МАТЕМАТИЧЕСКИ
СТУДИИ

Pliska Stud. Math. Bulgar. **17** (2005), 249–269

PLISKA
STUDIA MATHEMATICA
BULGARICA

PROBABILISTIC APPROACH TO DESIGN OF LARGE ANTENNA ARRAYS

Blagovest Shishkov, Hiroshi Matsumoto, Naoki Shinohara

Recent advances in space exploration have shown a great need for antennas with high resolution, high gain and low sidelobe (SL) level. The last characteristic is of paramount importance especially for the Microwave Power Transmission (MPT) in order to achieve higher transmitting efficiency. In this concern statistical methods play an important role. Various probabilistic properties of a large antenna array with randomly, uniformly and combined spacing of elements are studied and especially the relationship between the required number of elements and their appropriate spacing from one part and the desired SL level, the aperture dimension, the beamwidth and transmitting efficiency from the other. We propose a new unified approach in searching for reducing SL level by exploiting the interaction of deterministic and stochastic workspaces of proposed algorithms, emphasizing on the distribution of the maximums of SL level. These models indicate any advantages with respect to sidelobes in the large area around the main beam. A new concept of designing a large antenna array system is proposed. Our theoretic study and simulation results clarify how to deal with the problems of sidelobes in designing a large antenna array, which seems to be an important step toward the realization of future SPS/MPT systems.

2000 *Mathematics Subject Classification:* 78A50

Key words: microwave power transmission, large antenna array, uniform spacing, random spacing, spatial and amplitude tapering, sidelobe level, grating lobes, workspace, transmitting efficiency.

1. Introduction

In the 1980s and 1990s in Japan have performed large investigations on Solar Power Satellites (SPS) and Microwave Power Transmission (MPT), related by the abbreviations MINIX, ISY-METS, MILAX, SHARP, SPORTS and SPIRITZ [13]. In such way, the center of MPT technologies research shifted from USA to Japan. We will briefly consider how the problem of SL level was highlighted from previous investigators.

In his fundamental paper [24] T. Taylor studied the mathematical relationships involved in the radiation calculation of the line source from the point of view of function theory. Antenna design technique permits the other-than-uniform distributions of the field and in [24] has been investigated how to choose this distribution function to give a radiation pattern with prescribed properties such as, for example, narrow beamwidth of the main lobe and low sidelobes. In this original paper was documented the relationships between aperture edge behavior, far sidelobs, and array pattern zero locations. His analysis and insights led to a most practical technique for the synthesis of low-sidelobe beams.

A number of applications require a narrow scanned beam, but not commensurably high antenna gain. Since the array beamwidth is related to the largest dimension of the aperture, it is possible to remove many of the elements (or to "thin" an array) without significantly changing its beamwidth. For small or moderate arrays, it can be convenient to formulate the thinning procedure as a sidelobe minimization problem (see [26, 25, 17, 3]). In [26] the method is proposed of reducing both the quantities of elements required for a given size aperture and the number of different types of transmitters which would be necessary in an array using an illumination taper. In [25] a linear array with general arbitrarily distributed elements is discussed. A matrix relationship is found between the elements of the array and its far-zone pattern. In [17] general analytical expressions are presented for unequally spaced arrays. These relations allow for the analysis of the non-uniformly spaced array in terms of its equivalent uniformly spaced array. Some equivalence is made between the amplitude and spatial variation in the uniformly and non-uniformly spaced array. An array with monotonically increasing inter element spacing is presented as an example of the theory. In [3] a perturbation procedure for reducing the SL level of discrete linear arrays with uniform amplitude excitation by using non-uniform element spacing is presented. All these procedures [26, 25, 17, 3] do control both peak and average SL level, but are numerically difficult to implement for large antenna arrays.

The series of papers of Y. Lo [5-9 and 1] and especially the pioneering and fundamental paper [6] present probabilistic study of thinned antenna arrays. Lo

[6] addresses the peak-sidelobe issue and shows that a statistical description of these sidelobes is possible and yields useful bounds for array design. Taking into account this background we can draw the following conclusion:

1. For conventionally designed arrays where all elements are spaced uniformly, there exists an upper limit to the spacing if the grating lobes are not permitted to appear in the visible region.

2. Non-uniformly spaced algorithms are numerically difficult to implement for large antenna arrays.

3. Randomly spaced algorithms (the concept of "thin" arrays) are easier to implement, but need of further study in order to determine their merits and drawbacks.

In this paper we develop further the existing algorithms and propose new techniques to deal with sidelobes. This method can be used to predict the possible results for various sets of element spacings. This prediction can be made before carrying out detailed computations. The design of the array is thus reduced to playing a game in which the odds in favor of success are determined to be sufficiently large before any actual evaluation of the final array design is attempted.

2. Uniformly spaced arrays

Consider a linear array along the X axis in Cartesian coordinate system, Fig. 1. Suppose we are given N+1 equally excited antenna elements by isotropic radiation to be placed regularly within an aperture defined by $|X| \leq a/2$. In this case $\{X_n = nd_x\}$, where d_x is inter element distance usually measured in [m] or in wavelength.

$$d_x = p\lambda, \quad p = \pm 1, \pm 2, ...$$

Then for each vector $\{X_n\}$, $X_n \in R^{N+1}$, there is a radiation pattern function given by the magnitude of

$$P(\theta) = \frac{1}{N+1} \sum_{n=-N/2}^{N/2} \exp\left\{ j\frac{2\pi}{\lambda} (\sin\theta - \sin\alpha) \right\} nd_x \tag{1}$$

where

α—the scan angle measured from the normal to the array axis

θ–the observation angle measured from the normal to the array axis
$\{x_n = nd_x/N\}$ - normalized workspace
$a = Nd_x$ - the aperture, measured in [m]
Another representation will be used also

$$(2)\quad \begin{aligned} P(u) &= \tfrac{1}{N+1}\sum_{n=-N/2}^{N/2} \exp\{j2\pi(\sin\theta - \sin\alpha)\}nd_x \\ &= \tfrac{1}{N+1}\sum_{n=-N/2}^{N/2} \exp(jux_n) \end{aligned}$$

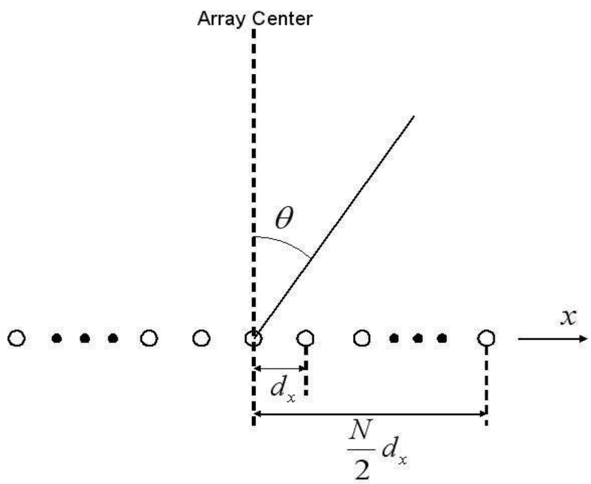

Figure 1: The structure of an uniform linear array with N elements

where
$u = a\pi(\sin\theta - \sin\alpha)$ – the observation angle parameter
$\{x_n = 2nd_x/N\}$ – normalized workspace
$a = Nd_x$ – the aperture, measured in wavelength
Let's denote $\frac{2\pi}{\lambda}(\sin\theta - \sin\alpha)\, nd_x = \psi_n$, then the array factor (AF) can be written as follows

$$(3)\quad |P(\theta)|^2 = \left| \frac{1}{N+1}\sum_{n=-N/2}^{N/2} e^{j\psi_n} \right|^2 = \frac{\sin^2[(N+1)\pi d_x(\sin\theta - \sin\alpha)/\lambda]}{(N+1)^2 \sin^2[\pi d_x(\sin\theta - \sin\alpha)/\lambda]}$$

A linear array with its peak at α can also have other peak values subject to the choice of spacing d_x. This ambiguity is apparent, since the summation also has a peak whenever the exponent is some multiple of 2π or

$$\frac{2\pi}{\lambda}\left(\sin\theta - \sin\alpha\right)d_x = 2\pi p, \quad p = \pm\left(1, 2, ...\right) \tag{4}$$

Such peaks are called grating lobes and are shown from the above to occur at angles θ_p such that

$$\sin\theta_p = \sin\alpha + \frac{p\lambda}{d_x}, \quad p = \pm\left(1, 2, ...\right) \tag{5}$$

for values of p that define an angle with a real sine ($|\sin\theta_p| \leq 1$). This imply that the maximum element spacing for an array scanned to a given angle α at frequency f is $\lambda/2$.

3. Randomly spaced array and distribution of its random pattern function at any observation point

Consider again the linear array of Fig. 1 and suppose we are given N+1 equally excited antenna elements by isotropic radiation to be placed at random within an aperture defined by $|X| \leq a/2$ in wavelength, in accordance with a common probability density function (pdf) $f\left(x\right)$.

Assume that the random positions $\{X_n\}$ are independent. Then for each sample vector $\{X_n\}$, $X_n \in R^{N+1}$, there is a sample radiation pattern function given by the magnitude of

$$\begin{aligned} P\left(u\right) &= \tfrac{1}{N+1}\sum_{n=-N/2}^{N/2} \exp\left\{j2\pi\left(\sin\theta - \sin\alpha\right)\right\}X_n \\ &= \tfrac{1}{N+1}\sum_{n=-N/2}^{N/2} \exp\left(jux_n\right) \end{aligned} \tag{6}$$

where the factor 1/N+1 is to insure that P(0)=1,

$u = a\pi\left(\sin\theta - \sin\alpha\right)$ – the observation angle parameter

$\{x_n = 2X_n/a\}$ – normalized workspace

$a = Nd_x$ – the aperture, measured in wavelength

In (6) if $\{X_n\}$ is considered as positions of conventional uniform spacing $\{X_n = nd_x\}$ the model is automatically transformed in the deterministic one – see (2). We will generalize the previous investigations by considering the mixed models when $\{X_n\}$ can be considered as sum of two vectors random one and deterministic one. Let's begin with a pure stochastic model which will be coded as Random Array 1 (RA 1). This model was first investigated by Y.T. Lo [6]. We can determine the Array Factor (AF) $|P(u)|^2$ as random function of u/π- see Fig. 2. Owing to the change of variable from X to x in (6), it follows that

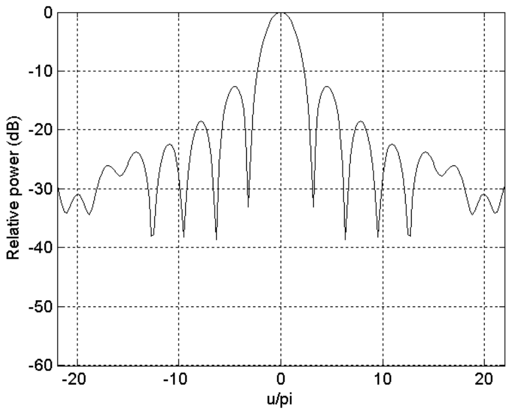

Figure 2: Radiation characteristics of RA 1 for N=1000

$f(x) \equiv 0$ for $|x| > 1$, and $\int\limits_{-1}^{1} f(x)dx = 1$

We have to determine the distribution of $|P(u)|$ at a given u (observation point). By taking the mathematical expectation of (6), one obtains

$$
\begin{aligned}
&E\{P(u)\} = (N+1)\,E\left\{\tfrac{1}{N+1}\exp(jux)\right\} \\
&= E\{\exp(jux)\} = \int\limits_{-\infty}^{\infty} f(x)\exp(jux)dx = \varphi(u)
\end{aligned}
\tag{7}
$$

where $\varphi(u)$ is the characteristic function of x.

It is seen that the mean pattern is identical to the pattern in Fig. 3, which would be obtained by taking $f(x)$ as a continuous aperture excitation. Since $f(x)$ has a finite support $[-1, 1]$, then $\varphi(u)$ is an integral transcendental function of the exponential type with exponent ≤ 1 and its asymptotic form ($|u| \to \infty$) was studied in [24]. In Fig. 4 is depicted the mean pattern $|\varphi(u)|^2$. Since the relations between the pattern function $\varphi(u)$ and the aperture excitation, being a Fourier transform pair, there is no difficulty in choosing a proper pdf $f(x)$ which will yield at least a desirable mean pattern.

Let $P_1(u)$ and $P_2(u)$ be the real and imaginary part of $P(u)$, which according to (6) is sum of independent random variables. By central limit theorem [2], the joint distribution of $P_1(u)$ and $P_2(u)$ is asymptotically normal. For simplicity

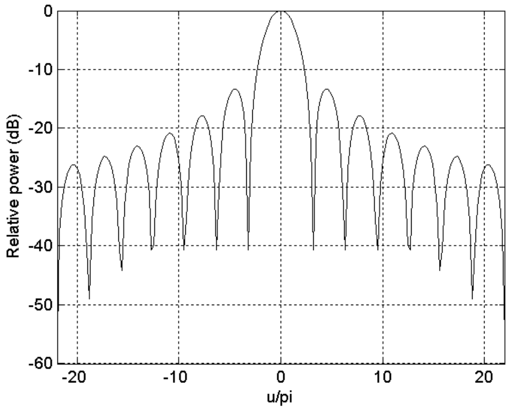

Figure 3: Mean radiation pattern of RA 1 for N=1000

let $f(x)$ be an even function, then their joint density function at each u is given by

(8) $$f(P_1, P_2) = \frac{1}{2\pi\sigma_1\sigma_2} \exp\left\{-\frac{1}{2}\left[\frac{(P_1-\varphi)^2}{\sigma_1^2} + \frac{P_2^2}{\sigma_2^2}\right]\right\}$$

where

$$\sigma_1^2(u) = E\left\{[P_1(u) - \varphi(u)]^2\right\} = \frac{1}{2N}[1 + \varphi(2u)] - \frac{1}{N}\varphi^2(u)$$

$$\sigma_2^2(u) = E\left\{P_2^2(u)\right\} = \frac{1}{2N}[1 - \varphi(2u)]$$

$$E\{P_1(u)\} = \varphi_1(u) = \varphi(u)$$

$$E\{P_2(u)\} = \varphi_2(u) = 0$$

Thus at any "u" the probability of antenna response being less than any level r is given by

(9) $$\Pr\{|P(u)| < r\} = \iint_{|P(u)|<r} f(P_1, P_2) dP_1 dP_2$$

This distribution is a generalized non-central chi-squared distribution with two degrees of freedom and concerns the entire visible range including the main beam area.

Two general opportunities were studied for the density function $f(x)$ of space tapering to be chosen and correspondent type of antenna amplitude excitation (illumination):

	Probability Density Function	Excitation Function
1.	$f(x) = \cos^2(\pi x/2)$ for $\lvert x\rvert \leq 1$ and $f(x) = 0$, otherwise.	1
2.	$f(x) = 1/2$ for $\lvert x\rvert \leq 1$ and $f(x) = 0$, otherwise.	$\cos^2(\pi x/2)$

We can determine the mean pattern $|\varphi(u)|^2$and variances $\sigma_1^2(u)$ and $\sigma_2^2(u)$ for each of the cases. In this paper we adopt the second case.

The determination of the distribution of the SL level in the entire visible range is equivalent to the determination of the maximum of the random function $|P(u)|$ for $u$in the above range excluding the main beam region. Since the random pattern function P(u) is analytic with probability 1, its probabilistic behavior can be determined by that of P(u) over only a denumerable set of u. In order to make the result more manageable numerically we may go one step further by studying its distribution over a finite set of u. For any u not in this set, the distribution of P(u) could be (at least in principal) interpolated from its Taylor's series expansion, since the distribution function and the covariance matrix of the derivative of P(u) are known.

Here an approximation will be made on the basis of the following argument. If $|P(u)|$ at a given u is less than a certain positive number r, then in its Δu-neighborhood $|P(u+\Delta u)|$ will be also less than r with a probability nearly equal to 1. This is due to a strong correlation between $P(u)$ and $P(u+\Delta u)$for (Δu) less than a certain value which turns out to be equal to the beamwidth (in u) of $\varphi(u)$, as can be seen from the covariance function $K(u,v)$ for large u, v.

Now let U' be the set of points u_n, where $|P(u_1)|, |P(u_2)|, \ldots$ are the sidelobe maxima in the entire visible range U. The distribution of $|P(u)|$ for u in the visible range is given by

$$\begin{aligned} &\Pr\{|P(u)| < r, u : \delta < |u| < 2\pi a\} = \Pr\{|P(u)| < r, u \in U'\} + \varepsilon \\ &\approx \quad \left[1 - \exp^{-Nr^2}\right]^{[4a]} \end{aligned} \tag{10}$$

where δ is the first positive zero of $\varphi(u)$ and ε is the error term. According to the above argument $|\varepsilon|$ is assumed to be small, while the first term on the right hand side of the above equation can be evaluated since $\{P(u_n)\}$ are jointly normal. Now for the sake of simplicity in numerical computation, one may introduce the following two step approximation. First one may regard $P(u_i)$ and $P(u_j)$ as independent for $i \neq j$ and then obtain a lower estimate

$$= \Pr\{|P(u)| < r, u \in U'\} \geq \prod_{n=1}^{[2a]} [\Pr\{|P(u_n)| < r\}]^2 \tag{11}$$

where $\varphi(u)$ is assumed to have $[2a]$ sidelobes for u in $0 < u < 2\pi a$ and $-2\pi a < u < 0$, respectively.

Second, consider the case of general interest where all the sidelobe maxima of the mean pattern $|\varphi(u_n)|$ are sufficiently smaller than r (i.e. r-max $|\varphi(u_n)|$ equal to two or three times of the standard deviation $\sigma = 1/\sqrt{2N}$). Then the right hand side of the above equation can be approximately computed by

$$[\Pr\{|P(\infty)| < r\}]^{[2a]} \tag{12}$$

where $P(\infty) = \lim_{u\to\infty} P(u)$. Since $E\{P(\infty)\} = 0$ and both $\sigma_1^2(u)$ and $\sigma_2^2(u)$ approach 1/2N as $u \to \infty$, $|P(\infty)|^2$ has a chi-square distribution with two degrees of freedom, namely

$$\Pr\{|P(\infty)| < r\} = 1 - e^{-Nr^2} \tag{13}$$

In short, let the aperture dimension $= 10^q$ wavelengths; then if ε is negligible one obtains the following approximate formula:

$$\begin{aligned} &\Pr\{|P(u)| < r, u : \delta < |u| < 2\pi a\} \\ &\approx \left[1 - \exp^{-Nr^2}\right]^{[4a]} = \left(1 - 10^{-0.4343Nr^2}\right)^{[4a]} \end{aligned} \tag{14}$$

This expression gives the number of elements required to achieve the desired SL level (maximum, not average) with predetermined confident probability of success such as 0.9, 0.95 etc. It is important to note, that for moderately large value of u, $\varphi(u) \approx 0, \sigma_1^2(u) \approx \sigma_2^2(u) \approx 1/2N$, independent of the pdf $f(x)$. This conclusion implies that although the pattern behavior in the main beam region is determined by $f(x)$, outside of the main beam area the variances are determined only by N, the number of elements, not the pdf $f(x)$. Therefore, in many cases (unless the near-in sidelobe level is of interest), it may be advantageous to us the uniform pdf for $f(x)$ to maintain a narrow beam. It is easy to extend this result on a rectangular aperture of $ab\lambda^2$ in the xy plane with a probability density function $f_1(x)\, f_2(y)$.

Let's compare this stochastic model RA 1 with the deterministic model of conventional uniform spacing UA model – Fig 4. One can make any important

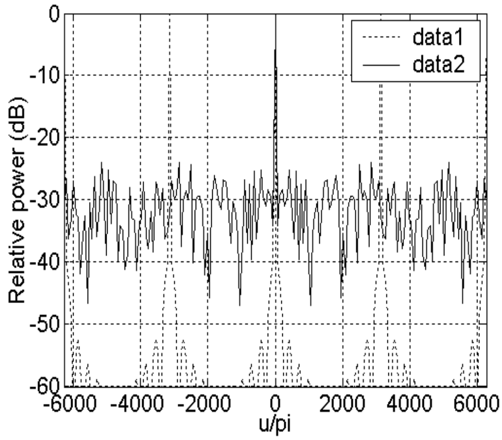

Figure 4: Radiation characteristics of RA 1 (data2) and UA (data1) with uniform excitation, N=1000

conclusion. In the entire visible range there is no grating lobes for RA 1. However the SL level is sufficiently high for random spacing of elements in comparison with uniform spacing – UA model. Second, from Fig. 2 we can see that the near SL level around the main beam is also sufficiently high for RA 1. All this has stimulated us to search for better solutions.

4. Mixed (combined) stochastic algorithm

The basic role of the algorithm for minimization of SL level play positions $\{X_n\}$ of antenna elements. This vector $\{X_n\}$, $X_n \in R^{N+1}$, or its normalized version $\{x_n\}$ creates the work space which plays a fundamental role. Generally $\{x_n\} = \{x_{n\,\det}\} + \{x_{nrand}\}$. Until now we have considered the models $\{x_{nrand}\}$ and $\{x_{n\,\det}\}$ that are called RA 1 and UA respectively.

In the terms of MATLAB

$$\{xnrand = rn = -1/2 + rand(1, N) \tag{15}$$

$$\{xndet = ((-N/2) : 1 : (N/2))/N\} \tag{16}$$

and each of the two workspaces operates over the interval [-1/2, 1/2].

Let's put forward the new model

$$RA2: \{x_n\} = \{x_{n\,\det}\} + \{\varepsilon_{nrand}\}, \quad \{\varepsilon_{nrand}\} = \{x_{nrand}\}/N \tag{17}$$

where $\{\varepsilon_{nrand}\}$ is a small random perturbation of the deterministic workspace and N is the number of elements. To compare all these models with respect to near and far SL level is more convenient to represent array factor

$$AF = |P(\theta)|^2 \tag{18}$$

or its averaged version as a function of observation angle θ.

So we can directly observe, that when N increases the beamwidth becomes narrower and the effect of broadening the beamwidth, when apply non-uniform amplitude tapering.

In the figures to be followed one depicts array factor $|P(\theta)|^2$ or its averaged version into the near zone around the main beam or entire visible range when changing any parameters. All the figures are prepared for f = 5.8 GHz and 181 observation points (N_{data}= 181) for which the array factor $|P(\theta)|^2$ is calculated. The scan angle α is adjusted to zero degree. The averaged version of the AF is obtained by repeating algorithm one hundred time and taking the mean operator of gathered statistics. All figures are prepared with uniform probability density function and with or without non-uniform amplitude excitation function.

We study the number of elements required as a function of the peak SL level (14) for various values of aperture a with a 90% probability of success.

We compare all stochastic algorithms (RA 1, RA 2,) with uniform array algorithm (UA) with $d_x = a/N$ (average spacing) and must clearly distinguish uniform spacing (deterministic) from non-uniform spacing with uniform pdf $f(x)$ (random).

In Fig. 5, one can see a comparison between the array factors of the our algorithm RA 2 with those of Lo's algorithm RA 1 in the near zone of the main beam, $\theta \in [-0.2°, 0.2°]$, $N = 1000$ and without amplitude tapering of element's excitation, or all elements (with isotropic radiation) are equally excited. There is no substantial difference between the deterministic and stochastic algorithms.

Now let's repeat Fig. 5 by applying a non-uniform excitation function of the kind $\cos^2(\pi x/2)$. In Fig. 6, one can see that in the near zone our algorithm RA 2, with non-uniform amplitude tapering, outperforms the Lo's algorithm RA 1 and broadening of beamwidth appears [7]. Its behavior is nearly the same as UA algorithm.

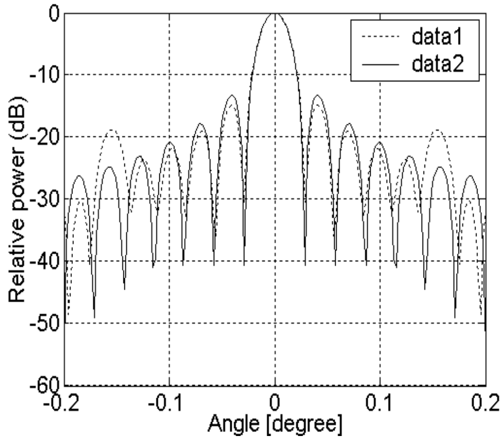

Figure 5: Radiation characteristics of RA 1 (data1) and RA 2 (data2), N=1000 and uniform excitation

A special attention deserves the algorithm RA 2 into the zone larger than that around the main beam $\theta \in [-15°, 15°]$, see Fig. 7 and Fig. 8. One can see a strong reduction of SL level in this zone. By applying amplitude tapering with $\cos^2(\pi x/2)$ this level becomes a little higher.

For the algorithm RA 2 and N=16000, 32000 and 64000 the average SL level decreases bellow -50dB respectively in the range of $\pm 6°$, $\pm 10°$, $\pm 15°$. It seems that this reduction of SL level is attractive for MPT.

5. Possibilities of using stochastic algorithms in MPT

Now let's increase number of elements N to 16000, 32000 and 64000. In Fig. 9 to Fig. 12 we fix again entire visible range and no amplitude tapering use.

One can see the influence of number of elements over peak SL level. For N=16000 elements this level according to (14) is bellow -35dB with 90% probability of success. When increasing this number to N=32000 and 64000 the peak SL level is bellow -37.5dB and -40dB respectively. So a large amount of elements need to decrease a little peak SL level. The average SL level for N=16000, N=32000 and N= 64000 is respectively -42dB, -45dB and -48dB – see Fig. 12.

To be determined the transmitting efficiency will be used the area under the average SL level and the area of main beam. When N increases, the area of main beam decreases, but average SL level decreases too. In Fig. 13 we turn back again to the near zone which becomes narrower and narrower when the number

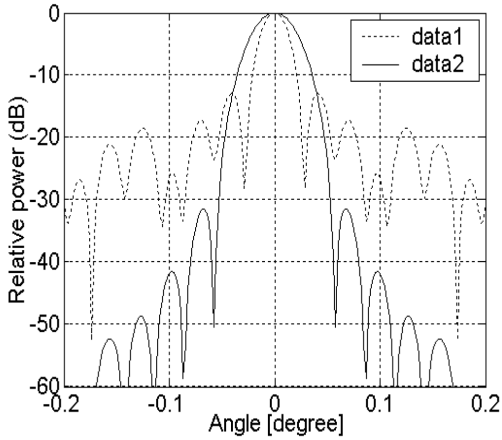

Figure 6: Radiation characteristics of RA 1 (data1) and RA 2 (data2), N=1000 and $\cos^2(\pi x/2)$ excitation

of element N increases. In this figure RA 1 and RA 2 are with non-uniform amplitude tapering with $\cos^2(\pi x/2)$. The transmitting efficiency was evaluated for RA 2 to be $\eta_{1D} = 0.4021$ and $\eta_{2D} = 0.1617$. The transmitting efficiency for RA 1 is lower. If we reduce deterministic work space two time the main beam enlarges and efficiency will be $\eta_{1D} = 0.5786$ and $\eta_{2D} = 0.3349$. Really the efficiency is bigger taking into account the strong reduction of SL level around the main beam and the participation of main beam area of several near sidelobes.

In the Table 1 are presented the features of the transmitting part of the system for MPT depend on number of elements and possible reduction of workspace.

Finally in Fig. 14 we propose a structure of a large antenna array according to our algorithm, see also [13].

Number of Antenna Elements	Number of PCM (=Sub-array)	Number of elements in Sub-array	Power [GW]	Diameter [m]	
				$d_{av} = \lambda$	$d_{av} = 2\lambda$
16000	1600	10	1.02	827	1654
32000	3200	10	4.1	1654	3308
64000	6400	10	16.38	3308	6616
128000	12800	10	65.5	6616	13232

Table 1: Characteristics of the transmitting part of the system for MPT

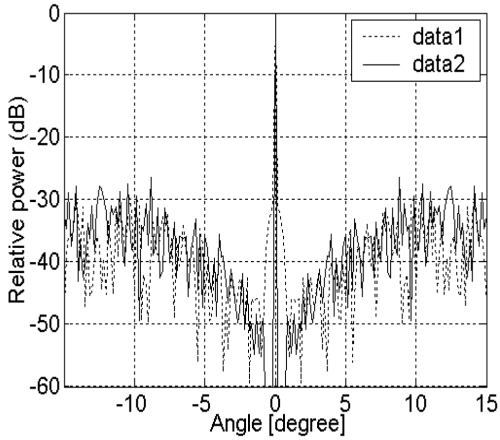

Figure 7: Radiation characteristics of the RA 2 for uniform excitation (data1) and $\cos^2(\pi x/2)$ excitation (data2), N=1000

Evidently, the design of such large linear array is unpractical for the MPT and as it has been mentioned at page 9 a square aperture has to be adopted $a^2\lambda^2$ with a probability density function $f_1(x)\, f_2(y)$. The measures of antenna area will be substantially reduced.

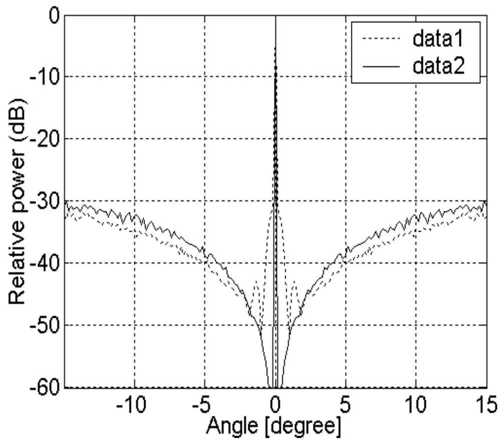

Figure 8: Average patterns of the RA 2 for uniform excitation (data1) and $\cos^2(\pi x/2)$ excitation (data2), N=1000

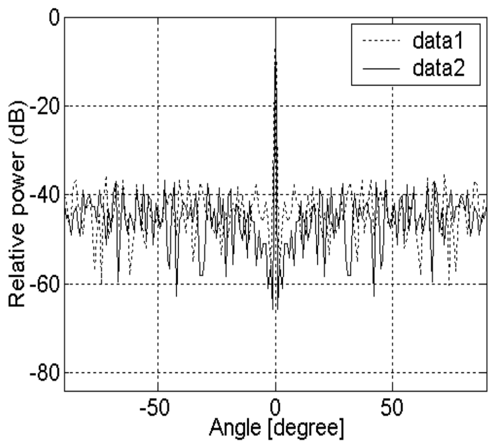

Figure 9: Radiation characteristics of the RA 1 (data1) and RA 2 (data2) with uniform excitation and N=16000, average spacing $d_{av} = 2\lambda$

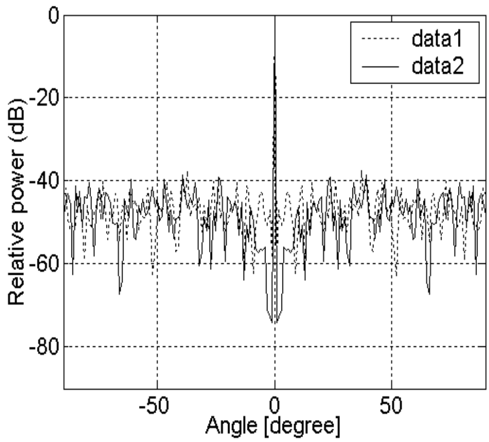

Figure 10: Radiation characteristics of the RA 1 (data1) and RA 2 (data2) with uniform excitation and N=32000, average spacing $d_{av} = 2\lambda$

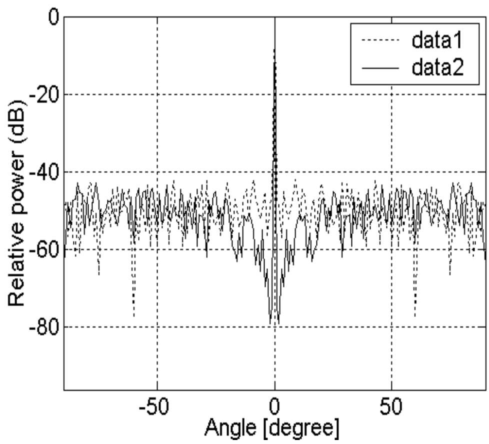

Figure 11: Radiation characteristics of the RA 1 (data1) and RA 2 (data2) with uniform excitation and N=64000, average spacing $d_{av} = 2\lambda$

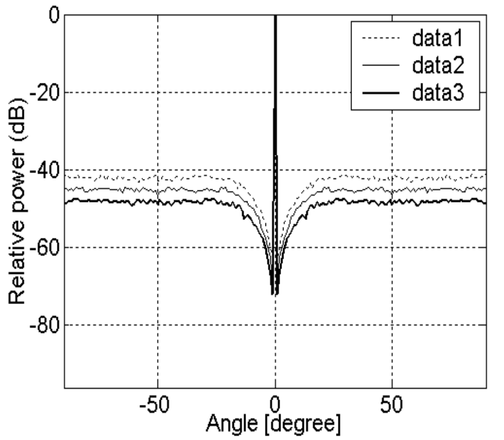

Figure 12: Average patterns of the RA 2 algorithm with uniform excitation for N=16000 (data 1), N=32000 (data 2) and N=64000 (data 3)

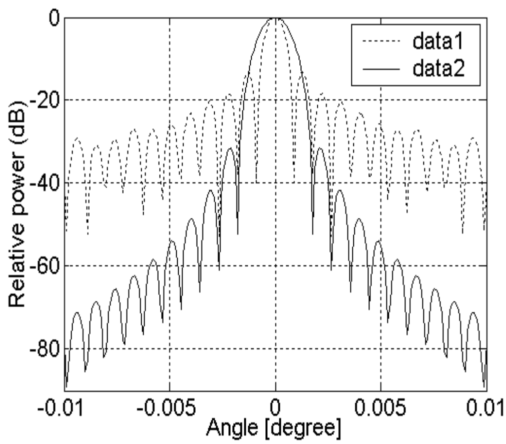

Figure 13: Radiation characteristics of the RA 1 (data1) and RA 2 (data2), N=32000, average spacing $d_{av} = 2\lambda$ with non-uniform excitation of$\cos^2(\pi x/2)$

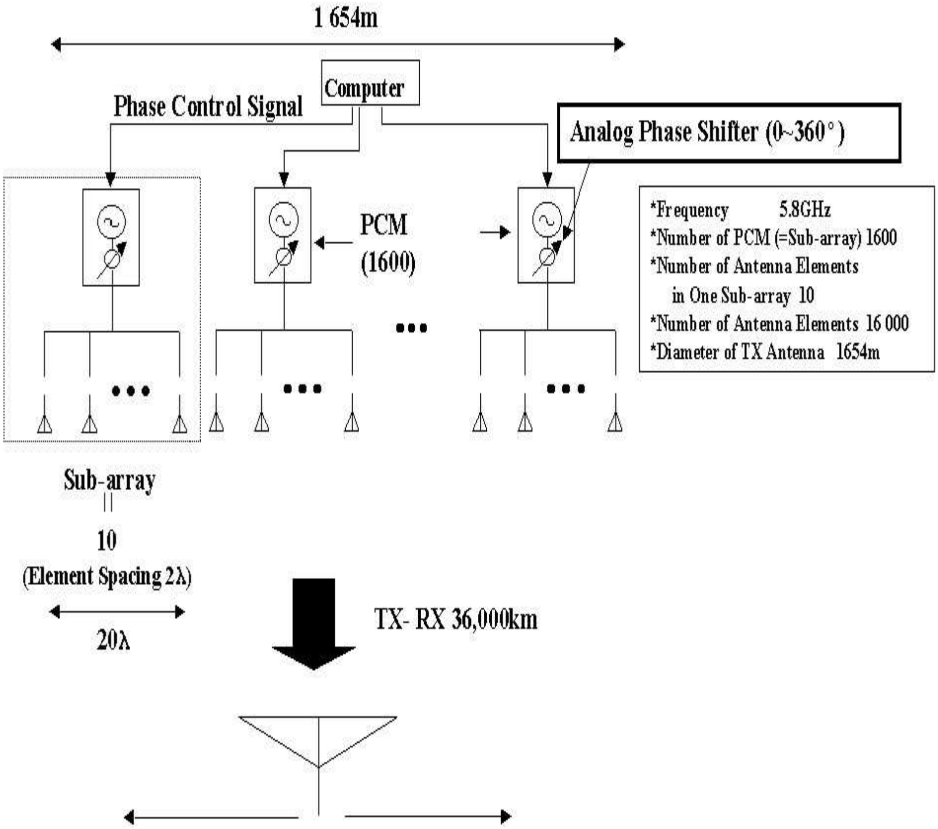

Figure 14: Structural scheme of the transmitting part of the system for MPT

6. Concluding remarks

For all stochastic algorithms

1. The number of elements required depends mainly on the desired sidelobe level. In general this number is less than that required from uniform spacing.

2. The resolution (or the beamwidth) depends mainly on the aperture dimension and to a lesser degree on the probability density function according to which the elements will be placed.

3. The directive gain is proportional to the number of elements used if the average spacing is large.

4. When the number of elements is fixed the resolution corresponding to an aperture can be improved considerably by spreading these elements over a larger aperture without great risk in obtaining a much higher sidelobe level and lower gain.

5. The interaction between deterministic and stochastic workspaces was exploited. Lo's algorithm is pure stochastic algorithm. Actually we perturb deterministic workspace with a little amount of random work space. As a result, there is no more grating lobes.

6. The proposed stochastic model RA 2 compete successfully the model RA 1 in the near sidelobe zone and take advantage with respect to SL level in the large area around the main beam.

7. According to our algorithm we propose a new concept of designing the transmitting part of the whole system for MPT.

With proposed algorithms we develop further the problem of reducing SL level of large antenna array systems which seems to be an important step toward the realization of future SPS/MPT systems.

REFERENCES

[1] Agrawal, V. D. and Y. T. Lo Mutual Coupling in Phased Arrays of Randomly Spaced Antennas *IEEE Trans. AP* **20(3)** May (1972), 288–295.

[2] Cramer, H. Mathematical Methods of Statistics. Princeton University Press, 1961.

[3] Harrington, R. F. Sidelobe Reduction by Nonuniform Element Spacing *IRE Trans. AP* **9** March (1961), 187–192.

[4] Hibino, T. and H. Matsumoto Study on the Array Factor of Non-uniform Array with Random Spacing *Radio Science Center for Space and Atmosphere* Kyoto University (2003), 1–9.

[5] Lo, Y. T. Sidelobe Level in Non-Uniformly Spaced Antenna Arrays *IEEE Trans. AP* **11** July (1963), 511–512.

[6] Lo, Y. T. A Mathematical Theory of Antenna Arrays with Randomly Spaced Elements *IEEE Trans. AP* **12** May (1964), 257–268.

[7] Lo, Y. T. High Resolution Antenna Arrays with Elements at Quantized Random Spacings *International Conference on Microwaves, Circuit Theory, and Information Theory* Tokyo (1964), 379–380.

[8] Lo, Y. T. and S. W. Lee A Study of Space-Tapered Arrays *IEEE Trans. AP* **14(1)** January (1966), 22–30.

[9] Lo, Y. T. and R. J. Simcoe An Experiment on Antenna Arrays with Randomly Spaced Elements *IEEE Trans. AP* **15(2)** March (1967) 231–235.

[10] Maher, T. M. and D. K. Cheng Random Removal of Radiators from Large Linear Arrays *IEEE Trans. AP* **11** March (1963) 106–112.

[11] Mailloux, R. J. and E. Cohen Statistically Thinned Arrays with Quantized Element Weights *IEEE Trans. AP* **39(4)** April (1991), 436–447.

[12] Mailloux, R. J. Phased Array Antenna Handbook. Artech House, Inc., 1994.

[13] Matsumoto, H. Research on Solar Power Satellites and Microwave Power Transmission in Japan *IEEE microwave magazine* December (2002), 36–45.

[14] McSpadden, J. O. and J. C. Mankins Space Solar Power Programs and Microwave Wireless Power Transmission Technology *IEEE microwave magazine* December (2002), 46–57.

[15] Numazaki, T., S. Mano, T. Kategi, and M. Mizusawa An Improved Thinning Method for Density Tapering of Planar Array Antennas *IEEE Trans. AP* **35(9)** Sept. (1987), 1066–1069.

[16] Papoulis, A. Probability, Random Variables, and Stochastic Processes. McGraw-Hill Book Company, 1965.

[17] Sandler, S. S. Some Equivalences Between Equally and Unequally Spaced Elements *IRE Trans. AP* **8** Sept. (1960), 496–500.

[18] Shinohara, N., H. Matsumoto, and K. Hashimoto Solar Power Station/Satellite (SPS) with Phase Controlled Magnetrons *IEICE Trans. Electron.* **E86-C(8)** August (2003), 1550–1555

[19] Shinohara, N., H. Matsumoto, and K. Hashimoto Solar Power Station/Satellite (SPS) with Phase Controlled Magnetrons *Radio Science Center for Space and Atmosphere* Kyoto University, (2002), 1–16.

[20] Shishkov, B., H. Tsuji, J. Xin, and Y. Hase Spatial and Temporal Processing of Cyclostationary Signals in Array Antennas Based on Linear Prediction Model *Proc. of the Telecommunications Advancement Organization (TAO) of Japan* (1988), 1–34.

[21] Shishkov, B., J. Cheng, and T. Ohira Adaptive Control Algorithm for the ESPAR Antenna Based on Stochastic Approximation Theory *IEICE Transactions on Communications* **E85-B(4)** April (2002), 802–811.

[22] Skolnik, M. I., J. W. Sherman III and F. C. Ogg, Jr. Statistically Designed Density-Tapered Arrays *IEEE Trans. AP* **12** July (1964), 408–417.

[23] Steinberg, B. D. Comparison Between the Peak Sidelobe of the Random Array and Algorithmically Designed Aperiodic Arrays *IEEE Trans. AP* **21** May (1973), 366–369.

[24] Taylor, T. T. Design of Line Source Antennas for Narrow Beamwidth and Low Sidelobes *IEEE Trans. AP.* **3** Jan. (1955), 16–28.

[25] Unz, H. Linear Arrays with Arbitrarily Distributed Elements *IRE Trans. AP* **8** March (1960), 222–223.

[26] Willey, R. E. Space Tapering of Linear and Planar Arrays *IRE Trans., AP* **10** July (1962), 369–377.

Blagovest Shishkov,
Institute of Mathematics
and Informatics
Bulgarian Academy of Sciences
Dept. of Telecommunications
Acad. G. Bontchev str., bl. 8
1113 Sofia, Bulgaria
e-mail:`bshishkov@math.bas.bg`

Hiroshi Matsumoto,
Naoki Shinohara
Research Institute
of Sustainable Humansphere
Kyoto University,
Uji, Japan
e-mail:`matsumot@rish.kyoto-u.ac.jp`
`shino@rish.kyoto-u.ac.jp`